This article has been accepted for publication in a future issue of this journal, but has not been fully edited. Content may change prior to final publication. Citation information: DOI 10.1109/ACCESS.2018.2820074, IEEE Access

Performance Analysis of Non-Orthogonal Multiple Access under I/Q Imbalance

Bassant Selim, *Student Member, IEEE*, Sami Muhaidat, *Senior Member, IEEE*, Paschalis C. Sofotasios, *Senior Member, IEEE*, Bayan S. Sharif, *Senior Member, IEEE*, Thanos Stouraitis, *Fellow, IEEE*, George K. Karagiannidis, *Fellow, IEEE*, and Naofal Al-Dhahir, *Fellow, IEEE*

***Abstract*—Non-orthogonal multiple access (NOMA) has been recently proposed as a viable technology that can potentially improve the spectral efficiency of fifth generation (5G) wireless networks and beyond. However, in practical communication scenarios, transceiver architectures inevitably suffer from radio-frequency (RF) front-end related impairments that can lead to degradation of the overall system performance with in-phase/quadrature-phase imbalance (IQI) constituting a major impairment in direct-conversion transceivers. In this article, we quantify the effects of IQI on the performance of NOMA based single-carrier (SC) and multi-carrier (MC) systems under multi-path fading conditions. This is realized by first deriving analytic expressions for the signal-to-interference-plus-noise ratio and the outage probability of both SC and MC NOMA systems subject to IQI at the transmitter and/or receiver (RX) side. Furthermore, we derive asymptotic diversity orders for all considered impairment scenarios. Capitalizing on these results, we demonstrate that the effects of IQI differ considerably among NOMA users and depend on the underlying systems' parameters. For example, for a target data rate and power allocation ratio satisfying a given condition, IQI does not affect the asymptotic diversity of SC NOMA systems whereas the asymptotic diversity of MC NOMA systems, suffering from RX IQI, is always zero. Moreover, it is shown that for both SC and MC NOMA systems, the first sorted user appears more robust to IQI, which indicates that higher order users are more sensitive to the considered impairment.**

***Index Terms*—Non-orthogonal multiple access, hardware impairments, I/Q imbalance, outage probability.**

B. Selim is with the Department of Electrical and Computer Engineering, Khalifa University of Science and Technology, PO Box 127788, Abu Dhabi, UAE (email: bassant.selim@kustar.ac.ae).

S. Muhaidat is with the Department of Electrical and Computer Engineering, Khalifa University of Science and Technology, PO Box 127788, Abu Dhabi, UAE and with the Institute for Communication Systems, University of Surrey, GU2 7XH, Guildford, UK (email: muhaidat@ieee.org).

P. C. Sofotasios is with the Department of Electrical and Computer Engineering, Khalifa University of Science and Technology, PO Box 127788, Abu Dhabi, UAE, and with the Department of Electronics and Communications Engineering, Tampere University of Technology, 33101 Tampere, Finland (e-mail: p.sofotasios@ieee.org).

B. Sharif is with the Department of Electrical and Computer Engineering, Khalifa University of Science and Technology, PO Box 127788, Abu Dhabi, UAE and with the School of Electrical and Electronic Engineering, Newcastle University, NE1 7RU, Newcastle upon Tyne, UK, (email: bayan@ieee.org).

T. Stouraitis is with with the Department of Electrical and Computer Engineering, Khalifa University of Science and Technology, PO Box 127788, Abu Dhabi, UAE and with the Department of Electrical and Computer Engineering, University of Patras, 265 04, Patras, Greece, (email: thanos.stouraitis@kustar.ac.ae).

G. K. Karagiannidis is with the Department of Electrical and Computer Engineering, Aristotle University of Thessaloniki, 54124 Thessaloniki, Greece (e-mail: geokarag@auth.gr).

N. Al-Dhahir is with the Department of Electrical Engineering, University of Texas at Dallas, TX 75080 Dallas, USA (e-mail: aldhahir@utdallas.edu).

I. Introduction

The emergence of the Internet of Things (IoT) together with the ever-increasing demands of mobile Internet impose high spectral efficiency and massive connectivity requirements on fifth generation (5G) wireless networks and beyond. Furthermore, future communication systems are expected to support heterogeneous devices with various service types, essential high throughput and low latency requirements. Based on this, non-orthogonal multiple access (NOMA) was recently introduced as an effective approach that is capable of overcoming these challenges, and thus rendering it a promising candidate for 5G systems. The distinct characteristic of NOMA is that it can be realized by allowing multiple users to share the same frequency bands and time slots through power-domain or code-domain multiplexing, while successive interference cancellation (SIC) is utilized to enable elimination of the resulting multi-user interference.

The key concept underlying NOMA is to make use of non-orthogonal resources, such as power or code-domain for multiple access (MA), instead of the time or frequency domain, as in orthogonal multiple access (OMA) schemes. Also, contrary to OMA schemes, NOMA does not allocate orthogonal resources to the different users and it instead performs SIC. Hence, NOMA can provide better spectral efficiency, higher cell-edge throughput and relaxed channel feedback as only the received signal strength is practically required. In addition, it is capable of providing low transmission latency since scheduling requests from users to the base station are not necessary [1]. Moreover, the number of supported users in OMA is strictly restricted to the amount of available resources, whereas the non-orthogonal resource allocation in NOMA can potentially lead to a significant increase of the number of connected devices in the network [2], [3].

A critical component of the massive number of interconnected devices is the radio frequency (RF) transceiver, which facilitates communication between the individual devices and/or their respective base stations. However, the continuously increasing demands in applications of RF transceivers has led to harsh design targets including increased performance and efficiency, low cost, low power dissipation, and small form factor. In this context, direct-conversion transceivers represent an effective RF front-end solution, as they demand neither external intermediate frequency filters nor image rejection filters. Hence, these transceiver architectures can be integrated on chip fairly easily while their cost is

rather low. However, in practical communication scenarios, these monolithic architectures suffer from inevitable RF front-end related imperfections due to components mismatch and manufacturing nonidealities, which limit the overall system performance. A critical example of these impairments is the in-phase (I)/quadrature-phase (Q) imbalance (IQI), which refers to the amplitude and phase mismatch between the I and Q branches of the transceiver, leading to imperfect image rejection, and ultimately resulting to performance degradation of the overall communication system [4], [5]. In ideal scenarios, the I and Q branches of a mixer have equal amplitude and a phase shift of 90°, providing an infinite attenuation of the image band; however, in practice, direct-conversion transceivers are sensitive to certain analog front-end related impairments that introduce errors in the phase shift as well as mismatches between the amplitudes of the I and Q branches which corrupt the down-converted signal constellation, thereby increasing the corresponding error rate [4].

I/Q signal processing is commonly realized in modern communication transceivers, which gives rise to the problem of matching the amplitudes and phases of the branches, and thus resulting in interference from the image signal [6]. Motivated by this practical concern, several recent works have attempted to model, mitigate or even exploit IQI, see [7]–[9] and the references therein. Specifically, the authors in [10] derive the signal-to-interference-plus-noise-ratio (SINR) taking into account the channel correlation between the subcarriers, in the context of orthogonal frequency division multiplexing (OFDM) systems. Assuming IQI at the receiver (RX) only, the SINR probability distribution function (PDF) of generalized frequency division multiplexing under Weibull fading channels was derived in [11] and was then used in the formulation of the corresponding average symbol error rate (SER) for the case of M-ary quadrature amplitude modulation. In the same context, the ergodic capacity of OFDM systems with RX IQI and single-carrier frequency-division-multiple-access systems with joint transmitter (TX)/RX IQI under Rayleigh fading conditions was investigated in [12] and [13], respectively. Likewise, the bit error rate (BER) of differential quadrature phase shift keying (DQPSK) was recently derived in [14] for single-carrier (SC) and multi-carrier (MC) systems in the presence of IQI. Moreover, the authors in [15] derived the SER of OFDM with $M-$QAM constellation, over frequency selective channels with RX IQI, whereas the authors in [16] quantified the effects of IQI on the outage probability of both SC and MC systems over cascaded Nakagami-m fading channels. Likewise, the error rate of subcarrier intensity modulated based QPSK over Gamma-Gamma fading channels with RX IQI was investigated in [17], while the impact of IQI on differential space time block coding (STBC)-based OFDM systems was recently analyzed in [18] and [19] by deriving an error floor and approximations for the corresponding BER. Finally, IQI has been also studied in half-duplex and full duplex amplify and forward (AF) and decode and forward cooperative systems [20]–[23], as well as in two-way relay systems and multi-antenna systems [24]–[28].

Despite the impact of RF front-end impairments on the system performance, their detrimental effect is often neglected. Therefore, it is necessary to investigate this topic, which even given its paramount importance for the actual realization of NOMA systems, it has not yet, to the best of the authors' knowledge, been addressed in the open technical literature [29]. Motivated by this, the present investigation is devoted to the quantification and analysis of the effects of IQI on NOMA based systems over multipath fading channels. Specifically, the main objective of this article is to develop a general framework for the comprehensive analysis of NOMA based systems under different IQI scenarios. To this end, a downlink NOMA system consisting of a base station (BS) and M users is considered. The cases of TX IQI only, RX IQI only and joint TX/RX IQI are formulated for both SC and MC transmission. Specifically, the SINR of both SC and MC NOMA systems in the presence of TX and/or RX IQI is derived. In order to quantify the effects of IQI on the considered NOMA based systems, the outage probability (OP) is used to evaluate the performance of the aforementioned impairments' scenarios. In more details, the main contributions of this work are summarized as follows:

- We derive novel analytic expressions for the SINR of SC and MC NOMA based systems over Rayleigh fading channels with TX and/or RX IQI along with novel closed form expressions for the corresponding SINR cummulative distribution function (CDF).
- We derive a unified closed form expression for the OP of SC NOMA systems under different impairment scenarios as well as OP expressions for MC NOMA systems subject to TX and/or RX IQI.
- For both SC NOMA and MC NOMA systems, under the different impairment scenarios considered, we derive the asymptotic diversity. We demonstrate that for SC NOMA systems and MC NOMA with TX IQI only, IQI does not affect the asymptotic diversity of the system as long as the target data rate satisfies a given condition.
- Extensive Monte-Carlo simulation results are presented in order to corroborate the derived exact and asymptotic expressions.

The remainder of the article is organized as follows: Section II presents the system model of the considered NOMA scenario and derives the SINR for both SC and MC systems subject to IQI. The OP and the asymptotic diversity orders of both SC and MC NOMA systems experiencing TX and/or RX IQI are derived in Section III. The corresponding numerical results for each considered scenario along with insights and discussions are provided in Section IV. Finally, closing remarks are given in Section V.

II. System Model

It is recalled that the basic idea behind NOMA is to allow a certain level of interference from adjacent users by allocating non-orthogonal resources to the different users in the network. In the present investigation, we consider the case of downlink NOMA where all users are served by a BS at the same time and frequency, but with different power levels. It is worth mentioning that power domain multiplexing NOMA can be efficiently realized by applying superposition coding at the TX and SIC at the RX. Hence, in order to serve several users

This article has been accepted for publication in a future issue of this journal, but has not been fully edited. Content may change prior to final publication. Citation information: DOI 10.1109/ACCESS.2018.2820074, IEEE Access

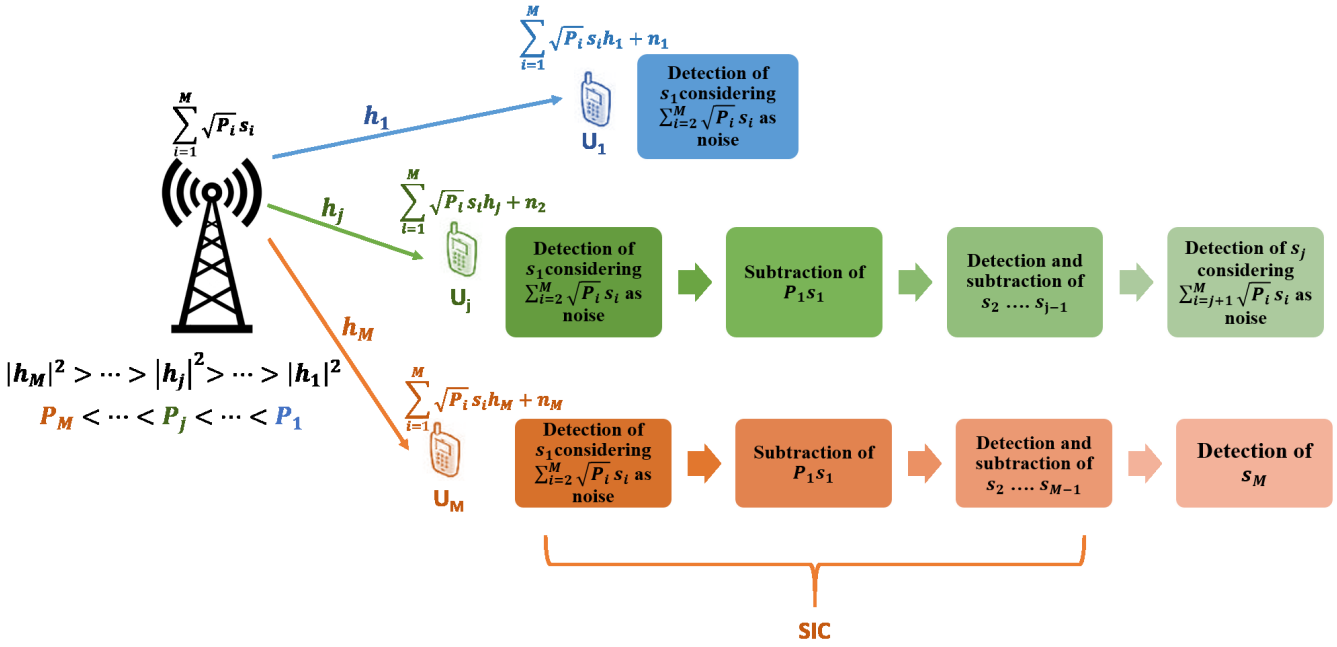

Fig. 1: Typical M user NOMA communication scenario.

simultaneously, the BS divides its transmission power between all users, while at the receiver end, multi-user detection is performed using SIC [2].

One of the key challenges in NOMA is how to allocate the power amongst the involved users. A common and fairly simple power allocation strategy is the fixed power allocation, where the power ratios are fixed and ordered according to the users' channel gains. In this scenario, we assume that more power is allocated to users with poorer channel conditions. In this context, we assume a single-cell NOMA downlink system consisting of a BS and M users, depicted in Fig. 1, with transceivers equipped with a single antenna. Based on this, we let h_i represent the small scale fading coefficient between the i^{th} user and the BS which follows a Rayleigh distribution. Therefore, for $|h_1|^2 \leq |h_2|^2 \leq ... \leq |h_M|^2$, and assuming an ideal RF front end, the baseband equivalent transmitted signal is given by [30]

$$x = \sum_{i=1}^{M} \sqrt{P_i} s_i \tag{1}$$

where $P_i = a_i E_t$ and s_i are the power and information symbol of the i^{th} sorted user, respectively. E_t is the transmit power of the BS, $\sum_{i=1}^{M} a_i = 1$ and $a_1 > a_2 > ... > a_M$. At the receiver RF front end, the received RF signal undergoes the necessary processing stages including filtering, amplification, analog I/Q demodulation (down-conversion) to baseband and sampling. Hence, assuming an ideal RF front end, the baseband equivalent received signal at the j^{th} sorted user is given by

$$r_j = h_j \sum_{i=1}^{M} \sqrt{P_i} s_i + n_j \tag{2}$$

where the subscript j refers to the j^{th} sorted user while h and n denote the channel coefficient and circularly symmetric complex additive white Gaussian noise (AWGN) signal, respectively. The j^{th} sorted user will then perform SIC in order to cancel the resulted interference for all users i, where $i < j$, whereas the signals intended for all other users with $i > j$ will be treated as noise. Hence, assuming perfect channel state information (CSI) and perfect cancellation, the instantaneous SINR per symbol of the m^{th} user's message at the j^{th} sorted user, $m < j$, is given by [31]

$$\gamma_{j \to m} = \frac{a_m}{\sum_{i=m+1}^{M} a_i + \frac{1}{\rho_j}} \tag{3}$$

where ρ_j is the j^{th} user's instantaneous signal-to-noise ratio (SNR) given by

$$\rho_j = \frac{E_t}{N_0} |h_j|^2 \tag{4}$$

where N_0 is the single-sided AWGN power spectral density.

It is noted here that the exact modeling and simulation of the RF front-end is typically complex and time consuming. Thus, applying baseband equivalent impairment models, instead of modeling the actual RF front-end, represents a pragmatic approach to the analysis of RF related impairments as this modeling relates the baseband representation to the bandpass signal with the RF impairments [32]. Based on this, we assume that the RF subcarriers in the present analysis are up/down converted to the baseband by direct conversion architectures and consider frequency independent IQI caused by the gain and phase mismatches of the I and Q mixers. Thus, the time-domain baseband representation of the IQI impaired signal is

given by [33]

$$g_{\text{IQI}} = \mu_{t/r} g_{\text{id}} + \nu_{t/r} g_{\text{id}}^{*} \tag{5}$$

where $(\cdot)^{*}$ denotes conjugation, g_{id} is the baseband IQI-free signal, g_{id}^{*} is due to IQI and the subscripts t/r denote the up/down-conversion process at the TX/RX, respectively. Furthermore, the IQI coefficients $\mu_{t/r}$ and $\nu_{t/r}$ are given by [32]

$$\mu_t = \frac{1}{2}\left(1 + \epsilon_t \exp\left(j\phi_t\right)\right), \tag{6}$$

$$\nu_t = \frac{1}{2}\left(1 - \epsilon_t \exp\left(-j\phi_t\right)\right), \tag{7}$$

$$\mu_r = \frac{1}{2}\left(1 + \epsilon_r \exp\left(-j\phi_r\right)\right) \tag{8}$$

and

$$\nu_r = \frac{1}{2}\left(1 - \epsilon_r \exp\left(j\phi_r\right)\right) \tag{9}$$

where $j = \sqrt{-1}$, whereas $\epsilon_{t/r}$ and $\phi_{t/r}$ are the TX/RX amplitude and phase mismatch levels, respectively. It is noted that for ideal RF front-ends, $\phi_{t/r} = 0^{\circ}$ and $\epsilon_{t/r} = 1$, which implies that $\mu_{t/r} = 1$ and $\nu_{t/r} = 0$. Moreover, the TX/RX image rejection ratio (IRR) is given by

$$\text{IRR}_{t/r} = \frac{\left|\mu_{t/r}\right|^2}{\left|\nu_{t/r}\right|^2} \tag{10}$$

where $|\cdot|$ denotes absolute value operation. It is noted that in SC systems, IQI causes distortion to the signal by its own complex conjugate while in MC systems, IQI causes distortion to the transmitted signal at subcarrier k by its image signal at subcarrier $-k$. In the following we present the signal model of both SC NOMA and MC NOMA based systems in the presence of IQI at the TX and/or RX.

A. Single-Carrier NOMA Systems Impaired by IQI

It is recalled that SC modulation is receiving considerable attention due to its robustness towards RF impairments compared to MC modulation [34]. As a result, it is increasingly rendered more suitable for low complexity and low power applications. In this context, this section presents the signal model and a comprehensive OP analysis for downlink SC NOMA based systems in the presence of TX and/or RX IQI effects.

1) TX Impaired by IQI: This case assumes that the RF front-end of the RX is ideal, while the TX experiences IQI. Based on this, for the case of an M user downlink NOMA system, the baseband equivalent transmitted signal is represented as

$$x_{\text{IQI}} = \mu_t \sum_{i=1}^{M} \sqrt{P_i} s_i + \nu_t \sum_{i=1}^{M} \sqrt{P_i} s_i^{*}. \tag{11}$$

where μ_t and ν_t correspond to the BS's IQI parameters and are given in (6) and (7), respectively. Hence, at the j^{th} sorted user, the baseband equivalent received signal is given by

$$r_{j_{\text{IQI}}} = \mu_t h_j \sum_{i=1}^{M} \sqrt{P_i} s_i + \nu_t h_j \sum_{i=1}^{M} \sqrt{P_i} s_i^{*} + n_j. \tag{12}$$

By also considering perfect CSI at the receiver, user j will perform SIC in order to cancel the interference from the $j-1$ users allocated more power than it, which under the assumption of perfect cancellation yields

$$\begin{aligned} r_{j_{\text{IQI}}} = {} & \left(\mu_t - 1\right) h_j \sum_{i=1}^{j-1} \sqrt{P_i} s_i + \mu_t h_j \sum_{i=j}^{M} \sqrt{P_i} s_i \\ & + \nu_t h_j \sum_{i=1}^{M} \sqrt{P_i} s_i^{*} + n_j. \end{aligned} \tag{13}$$

Hence, for $1 \leq m \leq j \leq M$, the instantaneous SINR per symbol of the m^{th} user's message at the j^{th} user is given by [35]

$$\frac{\mathbb{E}\left[\mu_t h_j \sqrt{P_m} s_m \left(\mu_t h_j \sqrt{P_m} s_m\right)^{*}\right]}{\mathbb{E}\left[\left(\Upsilon_j\right)\left(\Upsilon_j\right)^{*}\right]} \tag{14}$$

where $\mathbb{E}[\cdot]$ denote statistical expectation and

$$\begin{aligned} \Upsilon_j = {} & \left(\mu_t - 1\right) h_j \sum_{i=1}^{j-1} \sqrt{P_i} s_i + \mu_t h_j \sum_{i=j+1}^{M} \sqrt{P_i} s_i \\ & + \nu_t h_j \sum_{i=1}^{M} \sqrt{P_i} s_i^{*} + n_j. \end{aligned} \tag{15}$$

Finally, since $\sum_i^M a_i = 1$ and for $\mathbb{E}[s_i] = 0$, $\mathbb{E}[s_i s_k] = 0$ and $\mathbb{E}\left[s_i^2\right] = 0$, which is valid for most commonly used modulation schemes such as M-PSK and M-QAM, the instantaneous SINR per symbol of the m^{th} sorted user's message at the j^{th} sorted user's receiver is derived as

$$\gamma_{j \to m} = \frac{|\mu_t|^2 a_m}{|\mu_t - 1|^2 \sum\limits_{i=1}^{m-1} a_i + |\mu_t|^2 \sum\limits_{i=m+1}^{M} a_i + |\nu_t|^2 + \frac{1}{\rho_j}}. \tag{16}$$

2) RX Impaired by IQI: This case assumes that the RF front-end of the TX is ideal, while the RX is subject to IQI. Thus, for a M user downlink NOMA system, the baseband equivalent received signal at the j^{th} sorted user is expressed as

$$r_{j_{\text{IQI}}} = \mu_{r_j} h_j \sum_{i=1}^{M} \sqrt{P_i} s_i + \nu_{r_j} h_j^{*} \sum_{i=1}^{M} \sqrt{P_i} s_i^{*} + \mu_{r_j} n_j + \nu_{r_j} n_j^{*}. \tag{17}$$

where μ_{r_j} and ν_{r_j} correspond to the j^{th} user's IQI parameters and are given in (8) and (9), respectively. Similarly, assuming perfect CSI and perfect interference cancellation, following the SIC, one obtains

$$\begin{aligned} r_{j_{\text{IQI}}} = {} & \left(\mu_{r_j} - 1\right) h_j \sum_{i=1}^{j-1} \sqrt{P_i} s_i + \mu_{r_j} h_j \sum_{i=j}^{M} \sqrt{P_i} s_i \\ & + \nu_{r_j} h_j^{*} \sum_{i=1}^{M} \sqrt{P_i} s_i^{*} + \mu_{r_j} n_j + \nu_{r_j} n_j^{*}. \end{aligned} \tag{18}$$

Based on this, for $\mathbb{E}[s_i s_k] = 0$, the instantaneous SINR per

This article has been accepted for publication in a future issue of this journal, but has not been fully edited. Content may change prior to final publication. Citation information: DOI 10.1109/ACCESS.2018.2820074, IEEE Access

symbol of the m^{th} user's message at the j^{th} user is deduced, namely

$$\gamma_{j\to m}=\frac{|\mu_{r_j}|^2 a_m}{|\mu_{r_j}-1|^2\sum\limits_{i=1}^{m-1}a_i+|\mu_{r_j}|^2\sum\limits_{i=m+1}^{M}a_i+|\nu_{r_j}|^2+\frac{\Xi_{r_j}}{\rho_j}} \tag{19}$$

where $\Xi_{r_j}=|\mu_{r_j}|^2+|\nu_{r_j}|^2$.

3) Joint TX/RX impaired by IQI: This case assumes that both TX and RX are impaired by IQI. For a M user downlink NOMA system, the baseband equivalent received signal at the j^{th} sorted user is given by

$$\begin{aligned}r_{j_{\text{IQI}}}=&\left(\xi_{11_j}h_j+\xi_{22_j}h_j^*\right)\sum_{i=1}^{M}\sqrt{P_i}s_i\\&+\left(\xi_{12_j}h_j+\xi_{21_j}h_j^*\right)\sum_{i=1}^{M}\sqrt{P_i}s_i^*+\mu_{r_j}n_j+\nu_{r_j}n_j^*.\end{aligned} \tag{20}$$

where $\xi_{11_j}=\mu_{r_j}\mu_t$, $\xi_{22_j}=\nu_{r_j}\nu_t^*$, $\xi_{12_j}=\mu_{r_j}\nu_t$ and $\xi_{21_j}=\nu_{r_j}\mu_t^*$. Hence, assuming perfect CSI and perfect cancellation, following the SIC, one obtains

$$\begin{aligned}r_{j_{\text{IQI}}}=&\left(\left(\xi_{11_j}-1\right)h_j+\xi_{22_j}h_j^*\right)\sum_{i=1}^{j-1}\sqrt{P_i}s_i\\&+\left(\xi_{11_j}h_j+\xi_{22_j}h_j^*\right)\sum_{i=j}^{M}\sqrt{P_i}s_i\\&+\left(\xi_{12_j}h_j+\xi_{21_j}h_j^*\right)\sum_{i=1}^{M}\sqrt{P_i}s_i^*+\mu_{r_j}n_j+\nu_{r_j}n_j^*.\end{aligned} \tag{21}$$

Finally, following a similar approach as in II-A1, for $\mathbb{E}\left[s_i\right]=0$, $\mathbb{E}\left[s_is_k\right]=0$ and $\mathbb{E}\left[s_i^2\right]=0$, and after some mathematical manipulations, we obtain the instantaneous SINR per symbol of the m^{th} user's message at the j^{th} user receiver in (22), at the top of the next page.

Given that for direct conversion transceivers, the IRR is typically in the range of $20-40\text{dB}$ [16], it can be safely assumed that [36]

$$\left|\xi_{11_j}h\right|^2+\left|\xi_{22_j}h^*\right|^2\gg 2\Re\left[\xi_{11_j}h\xi_{22_j}^*h\right] \tag{23}$$

and

$$\left|\xi_{12_j}h\right|^2+\left|\xi_{21_j}h^*\right|^2\gg 2\Re\left[\xi_{12_j}h\xi_{21_j}^*h\right] \tag{24}$$

Hence, the SINR can be approximated as (25) at the top of the next page.

B. Multi-Carrier NOMA Systems Impaired by IQI

Although NOMA has demonstrated considerable capacity improvement and reduced latency, it suffers from several drawbacks, particularly, in small cells, where users could possibly experience similar channel conditions. In this respect, NOMA is envisioned to coexist with other OMA schemes, such as orthogonal frequency division multiple access (OFDMA), which will result in a significantly better overall performance and, potentially, fulfill the diverse requirements of different wireless services and applications [37]. It is recalled that MC systems are based on the division of the available signal bandwidth among K subcarriers, which has been shown to have several advantages such as enhanced robustness against multipath fading. Based on this, Long-Term Evolution (LTE) employs orthogonal frequency division multiplexing (OFDM), which is a MC modulation with orthogonal subcarriers, in the downlink.

In what follows, we derive the SINR CDF and the OP of MC NOMA systems in the presence of IQI assuming that the RF subcarriers are down converted to the baseband by wideband direct conversion. We also denote the set of subcarriers as

$$S=\left\{-\frac{K}{2},...,-1,1,...,\frac{K}{2}\right\} \tag{26}$$

and assume that there is an information signal present at the image subcarrier and that the channel responses at the k^{th} subcarrier and its image are uncorrelated.

1) TX Impaired by IQI: This case assumes that the RF front-end of the RX is ideal, while the TX experiences IQI. For the case of a M user downlink NOMA system, the baseband equivalent transmitted signal at the k^{th} subcarrier is given by

$$x_{\text{IQI}}\left(k\right)=\mu_t\sum_{i=1}^{M}\sqrt{P_i}s_i\left(k\right)+\nu_t\sum_{i=1}^{M}\sqrt{P_i}s_i^*\left(-k\right) \tag{27}$$

where the subcarrier $-k$ is the image of the subcarrier k. Based on this and assuming perfect CSI at the receiver, user j will perform SIC in order to cancel the interference from the users allocated a higher power ratio. Hence, for the case of perfect cancellation, it follows that

$$\begin{aligned}r_{j_{\text{IQI}}}\left(k\right)=&\left(\mu_t-1\right)h_j\left(k\right)\sum_{i=1}^{j-1}\sqrt{P_i}s_i\left(k\right)\\&+\mu_t h_j\left(k\right)\sum_{i=j}^{M}\sqrt{P_i}s_i\left(k\right)\\&+\nu_t h_j\left(k\right)\sum_{i=1}^{M}\sqrt{P_i}s_i^*\left(-k\right)+n_j\left(k\right).\end{aligned} \tag{28}$$

Based on this, following the SIC operation at the k^{th} subcarrier, the instantaneous SINR per symbol of the m^{th} user's message at the j^{th} user's receiver is represented as

$$\gamma_{j\to m}\left(k\right)=\frac{|\mu_t|^2 a_m}{|\mu_t-1|^2\sum\limits_{i=1}^{m-1}a_i+|\mu_t|^2\sum\limits_{i=m+1}^{M}a_i+|\nu_t|^2+\frac{1}{\rho_j(k)}}. \tag{29}$$

2) RX Impaired by IQI: This case assumes that the RF front-end of the TX is ideal, while the RX is subject to IQI. Following a similar approach, at the k^{th} subcarrier and the j^{th} sorted user, the baseband equivalent received signal is given

This article has been accepted for publication in a future issue of this journal, but has not been fully edited. Content may change prior to final publication. Citation information: DOI 10.1109/ACCESS.2018.2820074, IEEE Access

$$\gamma_{j\to m}=\frac{|\xi_{11_j}h_j+\xi_{22_j}h_j^*|^2a_m}{|\left(\xi_{11_j}-1\right)h_j+\xi_{22_j}h_j^*|^2\sum\limits_{i=1}^{m-1}a_i+|\xi_{11_j}h_j+\xi_{22_j}h_j^*|^2\sum\limits_{i=m+1}^{M}a_i+|\xi_{12_j}h_j+\xi_{21_j}h_j^*|^2+\frac{\Xi_{r_j}N_0}{E_t}} \tag{22}$$

$$\gamma_{j\to m}\approx\frac{\left(|\xi_{11_j}|^2+|\xi_{22_j}|^2\right)a_m}{\left(|\xi_{11_j}-1|^2+|\xi_{22_j}|^2\right)\sum\limits_{i=1}^{m-1}a_i+\left(|\xi_{11_j}|^2+|\xi_{22_j}|^2\right)\sum\limits_{i=m+1}^{M}a_i+|\xi_{12_j}|^2+|\xi_{21_j}|^2+\frac{\Xi_{r_j}}{\rho_j}}. \tag{25}$$

by

$$\begin{aligned}r_{j_{\text{IQI}}}(k)=&\mu_{r_j}h_j(k)\sum_{i=1}^{M}\sqrt{P_i}s_i(k)\\&+\nu_{r_j}h_j^*(-k)\sum_{i=1}^{M}\sqrt{P_i}s_i^*(-k)\\&+\mu_{r_j}n_j(k)+\nu_{r_j}n_j^*(-k).\end{aligned} \tag{30}$$

Therefore, assuming perfect CSI at the receiver and perfect cancellation, following the SIC, one obtains

$$\begin{aligned}r_{j_{\text{IQI}}}=&\left(\mu_{r_j}-1\right)h_j(k)\sum_{i=1}^{j-1}\sqrt{P_i}s_i(k)\\&+\mu_{r_j}h_j(k)\sum_{i=j}^{M}\sqrt{P_i}s_i(k)\\&+\nu_{r_j}h_j^*(-k)\sum_{i=1}^{M}\sqrt{P_i}s_i^*(-k)\\&+\mu_{r_j}n_j(k)+\nu_{r_j}n_j^*(-k).\end{aligned} \tag{31}$$

Finally, since $\mathbb{E}\left[h^2\right]=0$ and assuming $\mathbb{E}\left[s_is_k\right]=0$, at the k^{th} subcarrier, the instantaneous SINR per symbol for the m^{th} user's message at the j^{th} user is given by (32) at the top of the next page, where

$$\rho_j(-k)=\frac{E_t}{N_0|h_j(-k)|^2}. \tag{33}$$

3) Joint TX/RX Impaired by IQI: Here, we consider the case of MC NOMA where both the TX and RX suffer from IQI. To this effect, at the j^{th} user's receiver, the baseband equivalent received signal is given by

$$\begin{aligned}r_{j_{\text{IQI}}}=&\left(\xi_{11_j}h_j(k)+\xi_{22_j}h_j^*(-k)\right)\sum_{i=1}^{K}\sqrt{P_i}s_i(k)\\&+\left(\xi_{12_j}h_j(k)+\xi_{21_j}h_j^*(-k)\right)\sum_{i=1}^{K}\sqrt{P_i}s_i^*(-k)\\&+\mu_{r_j}n_j(k)+\nu_{r_j}n_j^*(-k).\end{aligned} \tag{34}$$

Hence, by also assuming perfect CSI and cancellation, following the SIC we obtain

$$\begin{aligned}r_{j_{\text{IQI}}}=&\left(\left(\xi_{11_j}-1\right)h_j(k)+\xi_{22_j}h_j^*(-k)\right)\sum_{i=1}^{j-1}\sqrt{P_i}s_i(k)\\&+\left(\xi_{11_j}h_j(k)+\xi_{22_j}h_j^*(-k)\right)\sum_{i=j}^{M}\sqrt{P_i}s_i(k)\\&+\left(\xi_{12_j}h_j(k)+\xi_{21_j}h_j^*(-k)\right)\sum_{i=1}^{M}\sqrt{P_i}s_i^*(-k)\\&+\mu_{r_j}n_j(k)+\nu_{r_j}n_j^*(-k).\end{aligned} \tag{35}$$

Similarly, since $\mathbb{E}\left[h^2\right]=0$ and assuming $\mathbb{E}\left[s_i\right]=0$, $\mathbb{E}\left[s_is_k\right]=0$, following a similar approach as in II-A3, at the k^{th} subcarrier, the instantaneous SINR per symbol of the m^{th} user's message at the j^{th} user's receiver is approximated (36), at the top of the next page.

III. OP OF NOMA WITH IQI

The OP can be defined as the probability that the symbol error rate is greater than a certain quality of service requirement and it can be computed as the probability that the SNR or SINR falls bellow a corresponding threshold which depends on the detection technique as well as on the modulation order [38]. In this section, assuming Rayleigh fading, we derive an analytical framework for the OP of SC NOMA and MC NOMA systems subject to the aforementioned IQI scenarios.

A. Single-carrier Systems

With the aid of (3), (16), (19) and (25), the SINR per symbol of the m^{th} user's message at the j^{th} sorted user's receiver can be expressed as

$$\gamma_{\text{IQI},j\to m}=\frac{\alpha_m}{\beta_m+\frac{A}{\rho_j}} \tag{37}$$

where the parameters α_m, β_m, and A depend on the considered impairment scenario and are depicted in Table I, at the top of the next page.

Proposition 1. *Assuming downlink SC NOMA systems with TX and/or RX IQI, the OP of the j^{th} sorted user is given by*

$$P_{\text{out},j}=\sum_{l=j}^{M}\binom{M}{l}\left[1-\exp\left(-\frac{\psi_m}{\overline{\gamma}}\right)\right]^l\left[\exp\left(-\frac{\psi_m}{\overline{\gamma}}\right)\right]^{M-l} \tag{38}$$

This article has been accepted for publication in a future issue of this journal, but has not been fully edited. Content may change prior to final publication. Citation information: DOI 10.1109/ACCESS.2018.2820074, IEEE Access

$$\gamma_{j\to m}(k)=\frac{|\mu_{r_j}|^2 a_m \rho_j(k)}{|\mu_{r_j}-1|^2\sum_{i=1}^{m-1}a_i\rho_j(k)+|\mu_{r_j}|^2\sum_{i=m+1}^{M}a_i\rho_j(k)+|\nu_{r_j}|^2\rho_j(-k)+|\mu_{r_j}|^2+|\nu_{r_j}|^2}. \tag{32}$$

$$\gamma_{j\to m}(k)\approx\frac{\left(|\xi_{11_j}|^2\rho_j(k)+|\xi_{22_j}|^2\rho_j(-k)\right)a_m}{\rho_j(k)\left(|\xi_{11_j}-1|^2\sum_{i=1}^{m-1}a_i+|\xi_{12_j}|^2+|\xi_{11_j}|^2\sum_{i=m+1}^{M}a_i\right)+\rho_j(-k)\left(|\xi_{22_j}|^2(1-a_m)+|\xi_{21_j}|^2\right)+\Xi_{r_j}}. \tag{36}$$

TABLE I: SC systems impaired by IQI parameters

	α_m	β_m	A
Ideal	a_m	$\sum_{i=1}^{m-1}a_i$	1
TX IQI	$\lvert\mu_t\rvert^2 a_m$	$\lvert\mu_t-1\rvert^2\sum_{i=1}^{m-1}a_i+\lvert\mu_t\rvert^2\sum_{i=m+1}^{M}a_i+\lvert\nu_t\rvert^2$	1
RX IQI	$\lvert\mu_{r_j}\rvert^2 a_m$	$\lvert\mu_{r_j}-1\rvert^2\sum_{i=1}^{m-1}a_i+\lvert\mu_{r_j}\rvert^2\sum_{i=m+1}^{M}a_i+\lvert\nu_{r_j}\rvert^2$	Ξ_{r_j}
Joint IQI	$\left(\lvert\xi_{11_j}\rvert^2+\lvert\xi_{22_j}\rvert^2\right)a_m$	$\left(\lvert\xi_{11_j}-1\rvert^2+\lvert\xi_{22_j}\rvert^2\right)\sum_{i=1}^{m-1}a_i+\left(\lvert\xi_{11_j}\rvert^2+\lvert\xi_{22_j}\rvert^2\right)\sum_{i=m+1}^{M}a_i+\lvert\xi_{12_j}\rvert^2+\lvert\xi_{21_j}\rvert^2$	Ξ_{r_j}

where $\overline{\gamma}=E_t/N_0$ is the average transmit SNR and

$$\psi_m=\max_{1\le m\le j}\frac{\phi_m A}{\alpha_m-\phi_m\beta_m}. \tag{39}$$

where $\phi_m=2^{R_m}-1$ and R_m is the targeted data rate of the m^{th} user [31]. Moreover, (38) is valid for

$$0\le\phi_m<\frac{\alpha_m}{\beta_m}, \tag{40}$$

otherwise $P_{\text{out},j}=1$.

Proof. The proof is provided in Appendix A. □

Capitalizing on Proposition 1, the asymptotic diversity order of SC NOMA with IQI is evaluated as [39]

$$d_a=\lim_{\overline{\gamma}\to\infty}\frac{-\log P_{\text{out}}}{\log\overline{\gamma}} \tag{41}$$

Since $\exp(-x)\underset{x\to 0}{\approx}1-x$, substituting (38) in (41), yields

$$d_e=\lim_{\overline{\gamma}\to\infty}\frac{-\log\left(\sum_{l=j}^{M}\binom{M}{l}\left(\frac{\psi_m}{\overline{\gamma}}\right)^l\left(1-\frac{\psi_m}{\overline{\gamma}}\right)^{M-l}\right)}{\log\overline{\gamma}}. \tag{42}$$

Moreover, since

$$\lim_{\overline{\gamma}\to\infty}\sum_{l=j}^{M}\binom{M}{l}\left(\frac{\psi_m}{\overline{\gamma}}\right)^l\left(1-\frac{\psi_m}{\overline{\gamma}}\right)^{M-l}=\lim_{\overline{\gamma}\to\infty}\binom{M}{j}\left(\frac{\psi_m}{\overline{\gamma}}\right)^j, \tag{43}$$

the asymptotic diversity can be approximated by

$$d_e=\lim_{\overline{\gamma}\to\infty}\frac{-\log\left(\binom{M}{j}\right)+j\left(\log(\overline{\gamma})-\log(\psi_m)\right)}{\log\overline{\gamma}} \tag{44}$$

$$=j \tag{45}$$

It is noted here that the above expression is only valid for ϕ_m satisfying the condition stated in (40), otherwise $P_{\text{out},j}=1$ and the asymptotic diversity is null. In addition, it is interestingly noticed that, for SC NOMA systems, the impairment scenario does not affect the asymptotic diversity, which is equal to the user's order.

B. Multi-Carrier Systems

1) TX Impaired by IQI: Here we assume MC transmission in the aforementioned downlink NOMA scenario where the TX only is impaired by IQI.

Proposition 2. *Assuming downlink MC NOMA systems with TX IQI only, the OP of the j^{th} sorted user is given by*

$$P_{\text{out},j}=\sum_{i=j}^{M}\binom{M}{i}\left[1-\exp\left(-\frac{\psi_m}{\overline{\gamma}}\right)\right]^i\left[\exp\left(-\frac{\psi_m}{\overline{\gamma}}\right)\right]^{M-i} \tag{46}$$

where ψ_m is given in (47), at the top the next page, while (46) is valid for

$$0\le\phi_m<\frac{|\mu_t|^2 a_m}{|\mu_t-1|^2\sum_{i=1}^{m-1}a_i+|\mu_t|^2\sum_{i=m+1}^{M}a_i+|\nu_t|^2}. \tag{48}$$

otherwise $P_{\text{out},j}=1$.

$$\psi_m = \max_{1\leq m\leq j} \frac{\phi_m}{|\mu_t|^2 a_m - \phi_m \left(|\mu_t - 1|^2 \sum_{i=1}^{m-1} a_i - |\mu_t|^2 \sum_{i=m+1}^{M} a_i + |\nu_t|^2 \right)} \tag{47}$$

Proof. Since (29) is similar to (16), it follows that the OP of MC NOMA system with TX IQI only is given by (46). □

Moreover, the asymptotic diversity of MC NOMA systems with TX IQI only is deduced from (45) for ϕ_m included in the range in (47) otherwise it is null.

2) RX Impaired by IQI: This case assumes that the RF front-end of the TX is ideal, while the RX is subject to IQI.

Proposition 3. *Assuming the aforementioned downlink MC NOMA system with RX IQI only, the OP of the j^{th} sorted user is expressed as*

$$P_{\text{out},j} = \sum_{l=j}^{M} \sum_{p=0}^{l} \binom{M}{l} \binom{l}{p} \frac{(-1)^p \exp\left(-\frac{\psi_m \Xi_{r_j}(M-l+p)}{\overline{\gamma}}\right)}{\left(1+\psi_m |\nu_{r_j}|^2 (M-l+p)\right)} \tag{49}$$

where

$$\psi_m = \max_{1\leq m\leq j} \frac{1}{\frac{|\mu_{r_j}|^2 a_m}{\phi_m} - |\mu_{r_j} - 1|^2 \sum_{i=1}^{m-1} a_i + |\mu_{r_j}|^2 \sum_{i=m+1}^{M} a_i} \tag{50}$$

while (49) is valid for

$$0 \leq \phi_m < \frac{|\mu_{r_j}|^2 a_m}{|\mu_{r_j} - 1|^2 \sum_{i=1}^{m-1} a_i + |\mu_{r_j}|^2 \sum_{i=m+1}^{M} a_i}. \tag{51}$$

otherwise, $P_{\text{out},j} = 1$.

Proof. The proof is provided in Appendix B. □

Substituting (49) in (41), the asymptotic diversity of MC NOMA systems with RX IQI only is obtained as

$$d_a = \lim_{\overline{\gamma}\to\infty} \frac{-\log\left(\sum_{l=1}^{M} \sum_{p=0}^{l} \binom{M}{l} \binom{l}{p} \frac{(-1)^p \left(1 - \frac{\psi_m \Xi_{r_j}(M-l+p)}{\overline{\gamma}}\right)}{\left(1+\psi_m |\nu_{r_j}|^2 (M-l+p)\right)} \right)}{\log \overline{\gamma}} \tag{52}$$

$$= 0. \tag{53}$$

which implies that for MC systems with RX IQI, an error floor is reached. This error floor can be obtained by taking $\overline{\gamma} = \infty$ in (49), yielding

$$P^{\infty}_{\text{out},j} = \sum_{l=j}^{M} \sum_{p=0}^{l} \binom{M}{l} \binom{l}{p} \frac{(-1)^p}{\left(1+\psi_m |\nu_{r_j}|^2 (M-l+p)\right)} \tag{54}$$

3) Joint TX/RX impaired by IQI: Here, we consider the case of MC NOMA where both the TX and RX experience IQI effects.

Proposition 4. *Assuming downlink MC NOMA systems with joint TX/RX IQI, the OP of the j^{th} sorted user is given by (55), at the top of the next page, where ψ_m is given in (56). moreover (55) is valid for*

$$0 \leq \phi_m < \frac{|\xi_{11_j}|^2 a_m}{|\xi_{11_j} - 1|^2 \sum_{i=1}^{m-1} a_i + |\xi_{11_j}|^2 \sum_{i=m+1}^{M} a_i + |\xi_{12_j}|^2} \tag{57}$$

If the above condition is not satisfied, the OP is 1.

Proof. The proof is provided in Appendix C. □

Substituting (55) in (41), the asymptotic diversity is obtained in (58). Importantly, this reveals that MC NOMA systems with joint TX/RX IQI asymptotically reach an error floor, regardless of the level of IQI considered. This error floor is obtained by taking $\overline{\gamma} = \infty$ in (55) yielding (59).

It is noted that in the above analysis we considered an ideal system where the users have perfect knowledge of the CSI. This is not usually the case in practice, and hence NOMA systems' performance is expected to further degrade under this condition. Hence, the present paper provides a lower bound to actual NOMA systems' OP performance. The analysis of imperfect CSI is out of the scope of this paper and can be found in [30].

IV. Numerical and Simulation Results

Considering the aforementioned NOMA approach, this section investigates the effect of TX and/or RX IQI on the performance of NOMA based communication systems. To this end and assuming Rayleigh fading conditions, extensive Monte Carlo simulations have been executed in order to investigate the OP performance of NOMA under IQI effects. It is noted that, unless otherwise stated, the number of users considered is $M = 2$ and that the power allocation coefficients are $a_1 = \frac{4}{5}$ and $a_2 = \frac{1}{5}$ for $M = 2$, and $a_1 = \frac{1}{2}$, $a_2 = \frac{1}{3}$ and $a_3 = \frac{1}{6}$ for $M = 3$ [31]. Moreover, for a fair comparison, we assume that the transmit power level is always fixed. This implies that the transmitted signal is normalized by $|\mu_t|^2 + |\nu_t|^2$ for TX IQI, by $|\mu_r|^2 + |\nu_r|^2$ for RX IQI and by $\left(|\mu_t|^2 + |\nu_t|^2\right)\left(|\mu_r|^2 + |\nu_r|^2\right)$ for joint TX/RX IQI. Figs. 2 − 5 and 6 − 8 present the OP of SC and MC NOMA based systems in the presence of IQI, respectively. It is noted that the numerical results are shown with solid lines, whereas markers are used to illustrate the respective computer simulation results. For both SC and MC systems, it is observed that the derived outage probability for TX and RX IQI only perfectly matches the simulations whereas for the case of joint TX/RX IQI, the proposed approximation accurately characterizes the system's outage probability.

This article has been accepted for publication in a future issue of this journal, but has not been fully edited. Content may change prior to final publication. Citation information: DOI 10.1109/ACCESS.2018.2820074, IEEE Access

$$P_{\text{out},j} = \sum_{l=j}^{M} \sum_{p=0}^{l} \binom{M}{l} \binom{l}{p} \frac{(-1)^p \exp\left(-\frac{\phi_m \Xi_{r_j} (M-l+p)\psi_m}{\overline{\gamma}}\right)}{\left(1+\psi_m (M-l+p)\left(\phi_m \left(|\xi_{22_j}|^2 (1-a_m) + |\xi_{21_j}|^2\right) - |\xi_{22_j}|^2 a_m\right)\right)}. \tag{55}$$

$$\psi_m = \max_{1 \le m \le j} \frac{1}{|\xi_{11_j}|^2 a_m - \phi_m \left(|\xi_{11_j} - 1|^2 \sum_{i=1}^{m-1} a_i + |\xi_{11_j}|^2 \sum_{i=m+1}^{M} a_i + |\xi_{12_j}|^2\right)}. \tag{56}$$

$$\begin{aligned} d_a &= \lim_{\overline{\gamma} \to \infty} \frac{-\log\left(\sum_{l=1}^{M} \sum_{p=0}^{l} \binom{M}{l} \binom{l}{p} \frac{(-1)^p \exp\left(-\frac{\phi_m \Xi_{r_j} (M-l+p)\psi_m}{\overline{\gamma}}\right)}{\left(1+\psi_m (M-l+p)\left(\phi_m \left(|\xi_{22_j}|^2 (1-a_m) + |\xi_{21_j}|^2\right) - |\xi_{22_j}|^2 a_m\right)\right)}\right)}{\log \overline{\gamma}} \\ &= 0. \end{aligned} \tag{58}$$

$$P^{\infty}_{\text{out},j} = \sum_{l=j}^{M} \sum_{p=0}^{l} \binom{M}{l} \binom{l}{p} \frac{(-1)^p}{\left(1+\psi_m (M-l+p)\left(\phi_m \left(|\xi_{22_j}|^2 (1-a_m) + |\xi_{21_j}|^2\right) - |\xi_{22_j}|^2 a_m\right)\right)}. \tag{59}$$

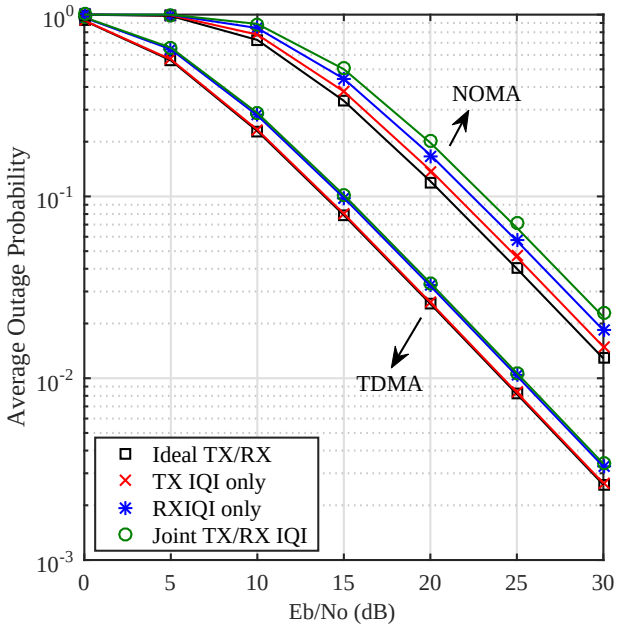

Fig. 2: Comparison between NOMA and TDMA in terms of the average OP for 3 user, $R = 0.9\,\text{bits/s/Hz}$ $\text{IRR}_t = \text{IRR}_r = 20\text{dB}$ and $\phi = 3°$.

A. SC NOMA Systems

The effects of TX IQI only, RX IQI only and joint TX/RX IQI on the OP performance of a 3 user NOMA based system compared to a 3 user time division multiple access (TDMA) based system are shown in Fig. 2. The considered IRR, which determines the amount of attenuation of the image frequency band, is 20dB. It is noted here that for a fair comparison, we fix the transmit power E_t. This implies that for NOMA, E_t is divided between the users during one time slot while for TDMA the transmit power is E_t/N_{users} for N_{users} time slots. The target data rate is $R = 0.9\,\text{bits/s/Hz}$. It is first observed that RX IQI has more detrimental impact on the system performance than TX IQI. This result is expected since RX IQI affects both the signal and the noise while TX IQI impairs the information signal only. Second, the detrimental effects of IQI are more pronounced for NOMA based systems compared to TDMA systems. In fact, while the average OP of TDMA seams uninfluenced by TX IQI and quite robust to RX IQI, NOMA observes some performance degradation, specially from RX IQI. This is explained by the fact that in NOMA, the power domain multiplexing causes interference not only from U_i's signal conjugate but from all the other NOMA users signal conjugate as well. Moreover, the interference cancellation performed by NOMA users does not take into account the IQI, leaving a portion of the signal uncanceled and since $a_1 > a_2 > ... > a_M$, this interference becomes significant as the number of users increase. This highlights the importance of modeling the effects of the well known RF impairments in the context of NOMA systems, where the power domain multiplexing as well as the SIC are ultimately expected to render the system more sensitive to RF impairments than OMA schemes.

Fig. 3 shows the OP as a function of the target data rate. We consider that the transmit SNR is $\gamma = 20\text{dB}$ and $\text{IRR}_t = \text{IRR}_r = 20\text{dB}$. Here, it is observed that the level of performance degradation caused by IQI depends on the target data rate, on the order of the considered sorted user and the incurred impairments. In fact, it is noticed that IQI affects U_2 more severely than U_1. This results from the SIC operation performed by U_2 without taking into account the IQI effects. Hence, following the SIC operation, U_2 is left

This article has been accepted for publication in a future issue of this journal, but has not been fully edited. Content may change prior to final publication. Citation information: DOI 10.1109/ACCESS.2018.2820074, IEEE Access

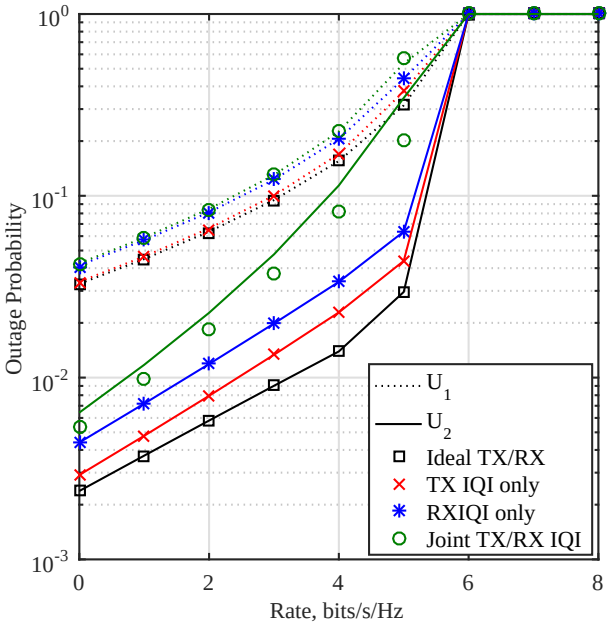

Fig. 3: SC system OP as a function of the target data rate for $\gamma = 20\text{dB}$, $\text{IRR}_t = \text{IRR}_r = 20\text{dB}$ and $\phi = 3°$.

with uncanceled interference from U_1. For instance, assuming $R = 2\,\text{bits/s/Hz}$, joint TX/RX IQI increases the OP of U_2 of more than 200% whereas U_1's OP is increased of around 33% only. Moreover, it is noticed that the target data rate also affects the level of performance degradation caused since, for U_2, the increase in the OP goes from 200% to almost 500% when increasing the rate from $2\,\text{bits/s/Hz}$ to $4\,\text{bits/s/Hz}$.

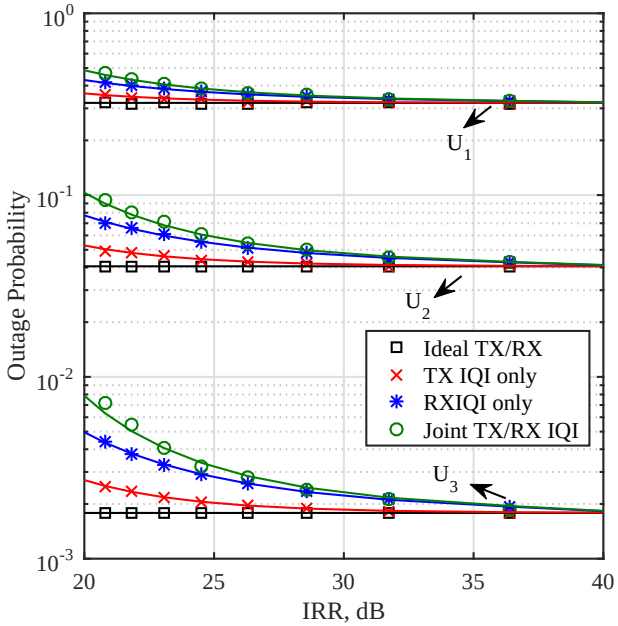

Fig. 4: SC system OP as a function of the normalized IRR for $R = 0.9\,\text{bits/s/Hz}$, $\gamma = 20\text{dB}$ and $\phi = 1°$.

In Fig. 4 the OP of a 3 user NOMA system is depicted as a function of the IRR for $\text{IRR}_t = \text{IRR}_r$, $\gamma = 25\text{dB}$ and $R = 0.95\,\text{bits/s/Hz}$. As mentioned earlier for a 2 user NOMA system, it is once more observed that IQI does not affect all the users equally. In fact, it is quite obvious that the performance degradation is directly proportional to the order of the user, i.e. to the number of SIC operations performed. Moreover, for the assumed scenario, the effects of IQI can be considered negligible for relatively high values of TX/RX IRR. Hence, this highlights the importance of the correct modeling of the effects of RF impairments, such as IQI on the performance of NOMA based systems. Furthermore, depending on the severity of the impairment, compensation techniques should be studied and implemented, if required, as in some cases the complexity engendered by compensation schemes is not justified with regards to the level of performance degradation caused.

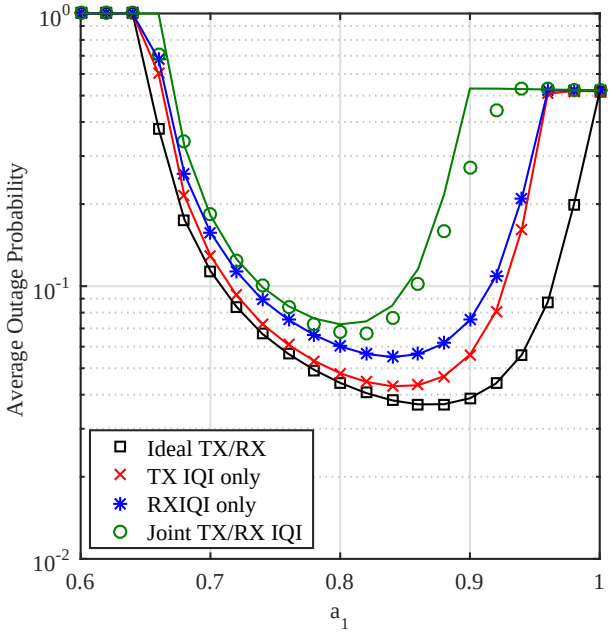

Fig. 5: SC system OP as a function of a_1 for $\gamma = 20\text{dB}$, $R = 1.5\,\text{bits/s/Hz}$, $\text{IRR}_t = \text{IRR}_r = 20\text{dB}$ and $\phi = 3°$.

In addition, the effects of IQI on the average OP for different power splitting ratios is depicted in Fig. 5. It is observed that, assuming $\gamma = 20\text{dB}$ and $R = 1.5\,\text{bits/s/Hz}$, the level of performance degradation caused by the impairment is also dependent upon the power splitting ratio. In fact, it is noticed that IQI can alter the optimum power splitting ratio that minimizes the average OP. This further highlights the importance of investigating the optimum power allocation taking into account RF impairments and/or the implementation of efficient dynamic compensation schemes.

B. MC NOMA Systems

Fig. 6 depicts the OP of MC NOMA systems as a function of the target rate for $\gamma = 20\text{dB}$ and $\text{IRR}_t = \text{IRR}_r = 20\text{dB}$. It is quite obvious that the effect of RX IQI is far more significant than TX IQI only. This is because TX causes interference from

This article has been accepted for publication in a future issue of this journal, but has not been fully edited. Content may change prior to final publication. Citation information: DOI 10.1109/ACCESS.2018.2820074, IEEE Access

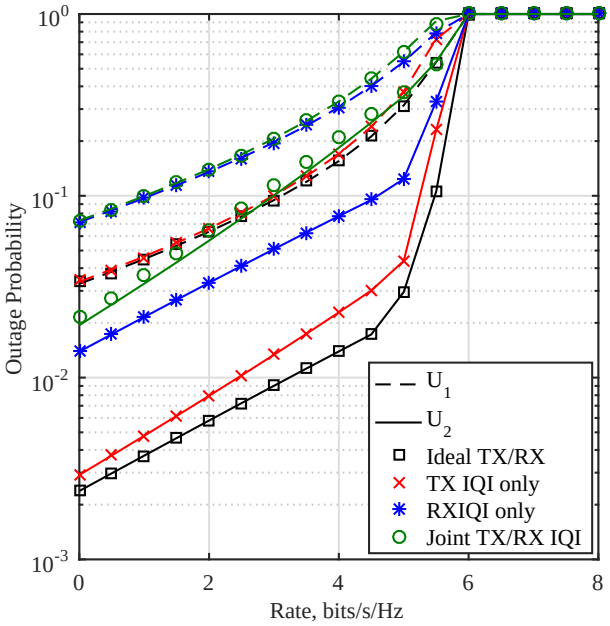

Fig. 6: MC system OP as a function of the target rate with $\mathrm{IRR}_t = \mathrm{IRR}_r = 20\mathrm{dB}$, $\gamma = 20\mathrm{dB}$ and $\phi = 3°$.

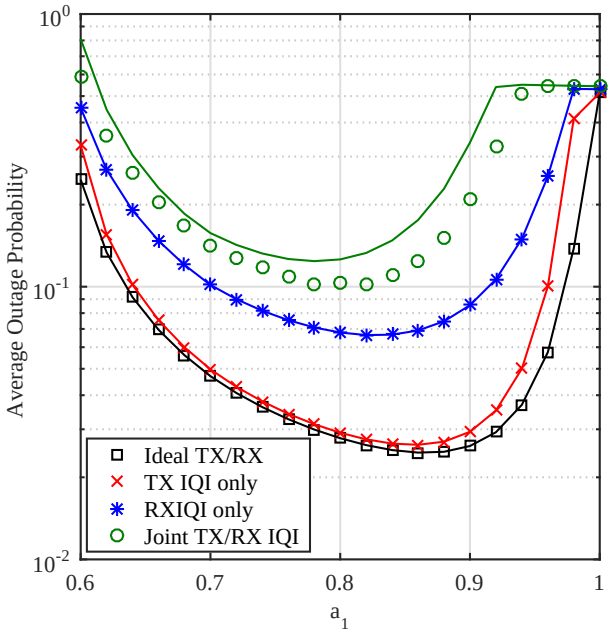

Fig. 7: MC system average OP as a function of a_1 for $\gamma = 20\mathrm{dB}$, $R = 1.25\,\mathrm{bits/s/Hz}$, $\mathrm{IRR}_t = \mathrm{IRR}_r = 20\mathrm{dB}$ and $\phi = 3°$.

the transmit signal only and not the noise or the channel gain as in RX IQI. This observation was made earlier for SC NOMA systems as well; however, it is observed that the gap between TX IQI only and RX IQI is even more significant for MC NOMA. For instance, for $R = 4\,\mathrm{bits/s/Hz}$ TX IQI increases the OP of U_2 by more than 110%, whereas RX IQI increases it by more than 980%.

Fig. 7 shows the average OP of MC NOMA systems for $R = 1.25\,\mathrm{bits/s/Hz}$. Once more, we observe the significant impact of RX IQI on MC NOMA based systems. In fact, we notice that both TX and RX IQI cause a relatively constant shift of the average OP where the performance penalty caused by TX IQI only is fairly small and could be neglected, whereas the effects of RX IQI are quite significant and require compensation in order to achieve a reliable communication link. Furthermore, once more, it is highlighted that this impairment can alter the optimum power allocation amongst the users.

Finally, Fig. 8 displays the OP of a 3 user MC NOMA system vs the IRR, assuming joint TX/RX IQI with $\mathrm{IRR}_t = \mathrm{IRR}_r$. For $R = 0.9\,\mathrm{bits/s/Hz}$ and $\gamma = 20\mathrm{dB}$, it is observed that, even though the level of OP increase depends on the user's index, IQI causes a quite significant degradation of the OP of all the NOMA users. In fact, for a relatively high IRR of $30\mathrm{dB}$, joint TX/RX IQI increases the OP of U_3 by nearly 68%, while U_1's OP is increased by approximately 13%.

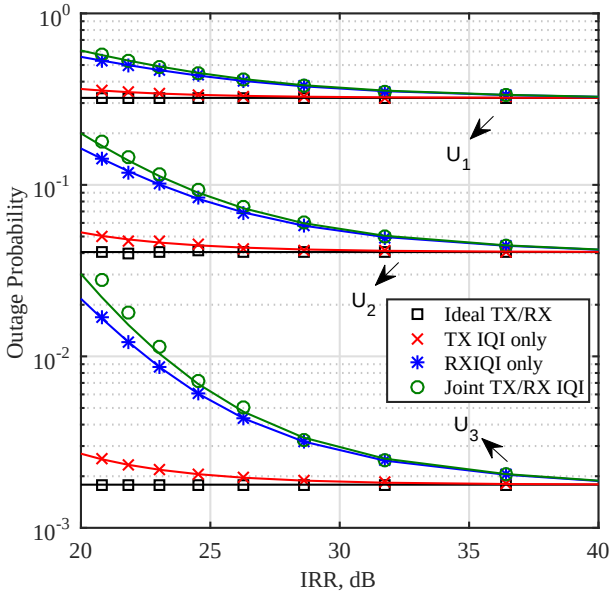

Fig. 8: MC system OP as a function of the IRR for 3 user NOMA system with $R = 0.9\,\mathrm{bits/s/Hz}$, $\gamma = 20\mathrm{dB}$, $\gamma = 25$ and $\phi = 1°$.

C. Comparison and Discussion

Fig. 9 shows the effects of RX IQI on a SC NOMA and a MC NOMA based system. It is observed that IQI causes a performance penalty in both systems; however, its impact is more significant in MC NOMA. More precisely, we observe that IQI causes a relatively constant shift of the OP in SC systems, whereas in MC NOMA, an OP floor is observed for all the users suffering from RX and consequently joint TX/RX IQI. This is in line with the derived asymptotic diversity order of 0, which confirms the analytical results derived in Section III-B. Moreover, for SC NOMA, with joint TX/RX IQI, Fig. 3 shows that the OP of U_2 is increased by 200% for $R = 2\,\mathrm{bits/s/Hz}$ whereas from Fig. 6, for the same rate

This article has been accepted for publication in a future issue of this journal, but has not been fully edited. Content may change prior to final publication. Citation information: DOI 10.1109/ACCESS.2018.2820074, IEEE Access

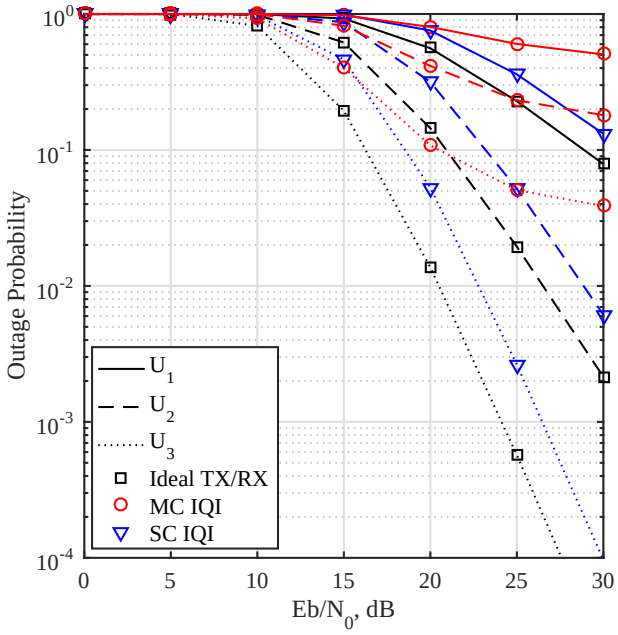

Fig. 9: Comparison between the effects of joint TX/RX IQI on SC and MC NOMA systems for 3 user with $R = 0.95\,\text{bits/s/Hz}$ $\text{IRR}_t = \text{IRR}_r = 20\text{dB}$ and $\phi = 3°$.

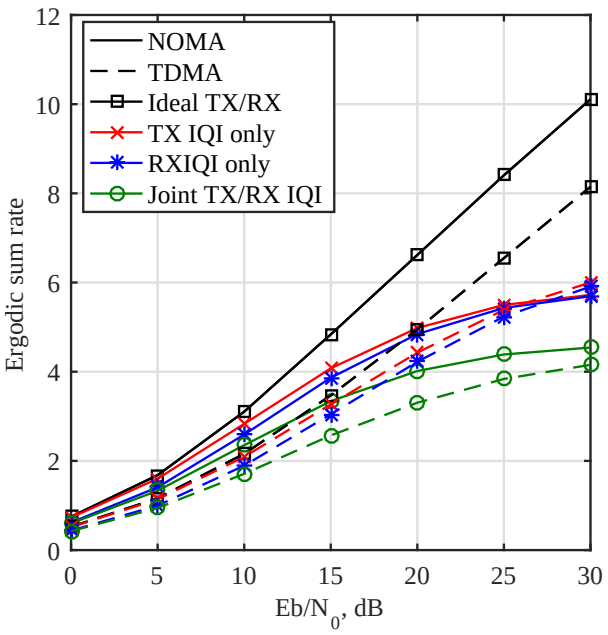

Fig. 10: Comparison between SC NOMA and TDMA in terms of the ergodic sum rate for 2 user, $\text{IRR}_t = \text{IRR}_r = 20\text{dB}$ and $\phi = 3°$.

and transmit SNR, MC NOMA systems' OP increases from 5.804×10^{-3} to 8.482×10^{-2} when subject to joint TX/RX IQI, which corresponds to an increase of more than 1350%. Similarly, in Fig. 4, it is shown that joint TX/RX IQI effects can increase U_3's OP by nearly 35% in SC NOMA systems whereas MC NOMA systems' OP witnesses an increase by more than 1600%. The reason underlying this is that in MC systems, IQI causes interference from the image subcarrier which affects the orthogonality of the system. Moreover, IQI in MC systems causes interference from the image subcarrier, which could benefit from better fading conditions than the desired signal, while SC IQI causes interference from the signal's own complex conjugate. Finally, in both SC and MC NOMA systems, it was shown in Figs. 5 and 7 that IQI can affect the optimum power allocation between the different NOMA users. Hence, the effective implementation of NOMA requires modeling of this impairment prior to the optimization of the system. Moreover, dynamic compensation, i.e. implemented by the users that are affected by the impairment only, can be effectively considered in order to avoid added complexity.

Finally, we compare the ergodic sum rate [31] of ideal and I/Q impaired SC and MC NOMA and TDMA systems in Figs. 10 and 11, respectively. The considered IRR is 20dB. Interestingly, in both cases, it is observed that the effect of IQI is more pronounced in the ergodic sum rate of NOMA than TDMA. Moreover, for the considered IQI levels, for SNR greater than 20dB, under joint TX/RX IQI, the ergodic sum rate of MC NOMA is lower than MC TDMA.

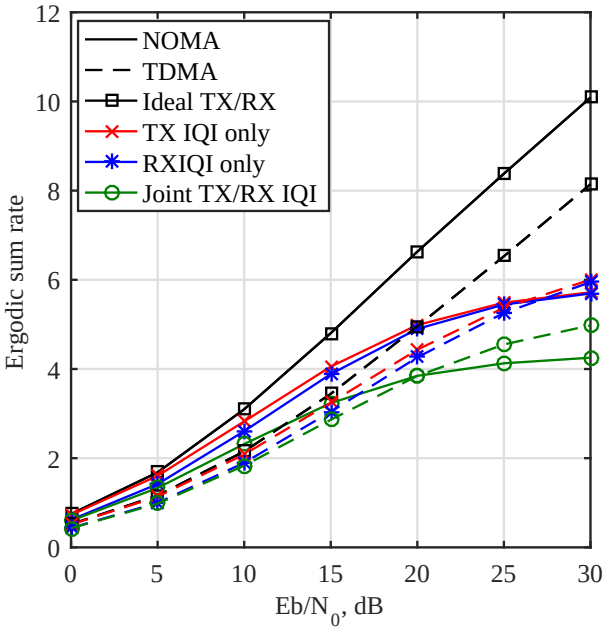

Fig. 11: Comparison between MC NOMA and TDMA in terms of the ergodic sum rate for 2 user, $\text{IRR}_t = \text{IRR}_r = 20\text{dB}$ and $\phi = 3°$.

V. Conclusion

We investigated the effects of IQI on the OP of both SC and MC NOMA based systems. The realistic cases of TX IQI only, RX IQI only and joint TX/RX IQI were considered and the corresponding OP over Rayleigh fading

This article has been accepted for publication in a future issue of this journal, but has not been fully edited. Content may change prior to final publication. Citation information: DOI 10.1109/ACCESS.2018.2820074, IEEE Access

channels was derived. In addition, the asymptotic diversity of both SC and MC NOMA systems was derived assuming all the different considered impairment scenarios. The derived analytic results were corroborated with respective results from computer simulations. It was shown that the level of performance degradation caused by IQI depends on numerous factors including the power allocation ratio, the impairment scenario, the target rate and the order of the considered user. This is due to the uncanceled interference from IQI that affects the performance of the employed SIC. Hence IQI affects SC NOMA based systems by affecting the SIC's performance while in MC NOMA systems both the SIC and the orthogonality of the subcarriers are compromised leading to more significant performance degradation. Moreover, it was shown that IQI can deviate the optimum power splitting ratio and hence compromise the efficiency of both SC and MC NOMA systems. To this end, this highlights the importance of effective modeling, optimization and dynamic compensation for the efficient implementation of the NOMA paradigm in future communication systems, such as 5G.

APPENDIX A
SC NOMA SYSTEMS IMPAIRED BY TX AND/OR RX IQI OP DERIVATION

It is highlighted that the j^{th} user is required to detect the messages intended for all users allocated a higher power ratio than itself before detecting its own message.

Without loss of generality, let the channel gains of all users be sorted in an ascending order as $|h_1|^2 \leq |h_2|^2 \leq ... \leq |h_M|^2$. Then, the power allocation coefficients are chosen such that $a_1 > a_2 > ... > a_M$. Assuming $1 < m < j$, the outage probability is defined as the probability that user j cannot detect its own signal or the signal intended for any user in the SIC ($j > m$), which is obtained as

$$P_{(out,j)} = 1 - \Pr\left\{E_{j\to 1}^{c} \bigcap \cdots \bigcap E_{j\to j}^{c}\right\} \tag{60}$$

where $E_{j\to m} = \{R_{j\to m} < R_m\}$ is the event that the j^{th} user cannot detect the m^{th} user's message, $R_{j\to m}$ denotes the rate for the j^{th} user to detect the m^{th} user's message, R_m is the targeted data rate of the m^{th} user and $E_{j\to m}^{c}$ the complementary set of $E_{j\to m}$ which can be written as

$$E_{j\to m}^{c} = \left\{\frac{\alpha_m}{\beta_m + \frac{A}{\rho_j}} > \phi_m\right\} \tag{61}$$

$$= \left\{\rho_j > \frac{\phi_m A}{\alpha_m - \phi_m \beta_m}\right\} \tag{62}$$

which is valid for $0 \leq \phi_m < \frac{\alpha_m}{\beta_m}$ and $\phi_m = 2^{R_m} - 1$. An outage event occurs at the j^{th} user if it is not able to decode its own message or the message of any of the users m in the SIC (i.e $m < j$). Hence, from (60), the OP of the j^{th} sorted user is obtained as as

$$P_{\text{out},j} = 1 - \Pr\{\rho_j > \psi_m\} \tag{63}$$

$$= F_{\rho_j}(\psi_m) \tag{64}$$

where $F_X(x)$ denote the CDF of X and ψ_m is given in (39). Making use of order statistics [40], the cumulative distribution function (CDF) of the j^{th} user's instantaneous SINR ρ_j is given by

$$F_{\rho_j}(x) = \begin{cases} \sum_{l=j}^{M} \binom{M}{l} [F_\rho(x)]^l [1 - F_\rho(x)]^{M-l}, & 0 \leq \phi_m < \frac{\alpha_m}{\beta_m} \\ 1, & \phi_m \geq \frac{\alpha_m}{\beta_m} \end{cases} \tag{65}$$

where F_ρ is the CDF of the unordered SNR which assuming Rayleigh fading, follows an exponential distribution. Hence, assuming TX and/or RX IQI, the OP of SC systems is obtained by (38).

APPENDIX B
MC NOMA SYSTEMS IMPAIRED BY RX IQI OP DERIVATION

Since the instantaneous SINR per symbol of the m^{th} user's message at the j^{th} user is given by (32), and following the same approach as in Appendix A, the conditional SINR CDF for a given $\rho_j(-k)$ is given by (66), at the top of the next page, which is valid for the range in (51). Meanwhile, for ϕ_m not satisfying (51), the OP is 1. Based on this, the unconditional CDF is obtained by integrating (66) over the distribution of $\rho_j(-k)$, namely the Rayleigh PDF in the considered scenario. Hence, expanding the binomial and after some mathematical manipulations, equation (67) is deduced. Finally, by evaluating the involved integral and recalling that an outage event occurs at the j^{th} user if it is not able to decode its own message or the message of any of the users m in the SIC (i.e $m < j$), the OP in (49) is deduced, which completes the proof.

APPENDIX C
MC NOMA SYSTEMS IMPAIRED BY JOINT TX/RX IQI OP DERIVATION

Considering the instantaneous SINR per symbol of the m^{th} user's message at the j^{th} user given in (36), for a given $\rho_j(-k)$, following the same approach as in Appendix B, the conditional SINR CDF is given by (68) and is valid for the range presented in (57), while for ϕ_m not satisfying (57), the OP is 1.

Based on this, the unconditional CDF is obtained following the same approach as in Appendix C. Hence, expanding the binomial, performing some mathematical manipulations and solving the integral, yields (55), which completes the proof.

REFERENCES

[1] S. M. R. Islam, N. Avazov, O. A. Dobre, and K. S. Kwak, "Power-domain non-orthogonal multiple access (NOMA) in 5G systems: Potentials and challenges," *IEEE Commun. Surveys Tuts*, vol. 19, no. 2, pp. 721–742, Secondquarter 2017.

[2] L. Dai, B. Wang, Y. Yuan, S. Han, C. l. I, and Z. Wang, "Non-orthogonal multiple access for 5G: solutions, challenges, opportunities, and future research trends," *IEEE Commun. Mag.*, vol. 53, no. 9, pp. 74–81, Sep. 2015.

[3] Y. Yuan, Z. Yuan, G. Yu, C. H. Hwang, P. K. Liao, A. Li, and K. Takeda, "Non-orthogonal transmission technology in LTE evolution," *IEEE Commun. Mag.*, vol. 54, no. 7, pp. 68–74, July 2016.

This article has been accepted for publication in a future issue of this journal, but has not been fully edited. Content may change prior to final publication. Citation information: DOI 10.1109/ACCESS.2018.2820074, IEEE Access

$$F_{\rho_{j\to m}}\left(\phi_m|\rho_j\left(-k\right)\right)=\sum_{l=1}^{M}\binom{M}{l}\left(1-\exp\left(-\frac{\phi_m}{\overline{\gamma}}\frac{\left(|\nu_{r_j}|^2\rho_j\left(-k\right)+\Xi_{r_j}\right)}{|\mu_{r_j}|^2a_m-\phi_m\left(|\mu_{r_j}-1|^2\sum\limits_{i=1}^{m-1}a_i+|\mu_{r_j}|^2\sum\limits_{i=m+1}^{M}a_i\right)}\right)\right)^{l}\times\left(\exp\left(-\frac{\phi_m}{\overline{\gamma}}\frac{\left(|\nu_{r_j}|^2\rho_j\left(-k\right)+\Xi_{r_j}\right)}{|\mu_{r_j}|^2a_m-\phi_m\left(|\mu_{r_j}-1|^2\sum\limits_{i=1}^{m-1}a_i+|\mu_{r_j}|^2\sum\limits_{i=m+1}^{M}a_i\right)}\right)\right)^{M-l}. \tag{66}$$

$$F_{\rho_{j\to m}}\left(\phi_m\right)=\sum_{l=1}^{M}\sum_{p=0}^{l}\binom{M}{l}\binom{l}{p}\left(-1\right)^p\int_0^{\infty}\exp\left(-\frac{\phi_m}{\overline{\gamma}}\frac{p\left(|\nu_{r_j}|^2y+\Xi_{r_j}\right)}{|\mu_{r_j}|^2a_m-\phi_m\left(|\mu_{r_j}-1|^2\sum\limits_{i=1}^{m-1}a_i+|\mu_{r_j}|^2\sum\limits_{i=m+1}^{M}a_i\right)}\right)\times\exp\left(-\frac{\phi_m}{\overline{\gamma}}\frac{\left(M-l\right)\left(|\nu_{r_j}|^2y+\Xi_{r_j}\right)}{|\mu_{r_j}|^2a_m-\phi_m\left(|\mu_{r_j}-1|^2\sum\limits_{i=1}^{m-1}a_i+|\mu_{r_j}|^2\sum\limits_{i=m+1}^{M}a_i\right)}\right)\frac{\exp\left(-\frac{y}{\overline{\gamma}}\right)}{\overline{\gamma}}dy. \tag{67}$$

$$F_{\rho_{j\to m}}\left(\phi_m|\rho_j\left(-k\right)\right)=\sum_{l=1}^{M}\binom{M}{l}\left(1-\exp\left(-\frac{\phi_m\rho_j\left(-k\right)\left(|\xi_{22_j}|^2\left(1-a_m\right)+|\xi_{21_j}|^2\right)+\phi_m\Xi_{r_j}-|\xi_{22_j}|^2\rho_j\left(-k\right)a_m}{\overline{\gamma}\left(|\xi_{11_j}|^2a_m-\phi_m\left(|\xi_{11_j}|^2\left(1-a_m\right)+|\xi_{12_j}|^2-\sum\limits_{i=m+1}^{M}a_i\right)\right)}\right)\right)^{l}\times\left(\exp\left(-\frac{\phi_m\rho_j\left(-k\right)\left(|\xi_{22_j}|^2\left(1-a_m\right)+|\xi_{21_j}|^2\right)+\phi_m\Xi_{r_j}-|\xi_{22_j}|^2\rho_j\left(-k\right)a_m}{\overline{\gamma}\left(|\xi_{11_j}|^2a_m-\phi_m\left(|\xi_{11_j}|^2\left(1-a_m\right)+|\xi_{12_j}|^2-\sum\limits_{i=m+1}^{M}a_i\right)\right)}\right)\right)^{M-l}. \tag{68}$$

[4] S. Mirabbasi and K. Martin, "Classical and modern receiver architectures," *IEEE Commun. Mag.*, vol. 38, no. 11, pp. 132–139, Nov 2000.

[5] S. Bernard, "Digital communications fundamentals and applications," *Prentice Hall, USA*, 2001.

[6] M. Valkama, M. Renfors, and V. Koivunen, "Advanced methods for I/Q imbalance compensation in communication receivers," *IEEE Trans. Signal Process.*, vol. 49, no. 10, pp. 2335–2344, Oct 2001.

[7] O. Ozdemir, R. Hamila, and N. Al-Dhahir, "I/Q imbalance in multiple beamforming OFDM transceivers: SINR analysis and digital baseband compensation," *IEEE Trans. Commun.*, vol. 61, no. 5, pp. 1914–1925, May 2013.

[8] B. Selim, P. C. Sofotasios, S. Muhaidat, and G. K. Karagiannidis, "The effects of I/Q imbalance on wireless communications: A survey," in *2016 IEEE 59th International Midwest Symposium on Circuits and Systems (MWSCAS)*, Oct 2016, pp. 1–4.

[9] R. Hamila, O. Ozdemir, and N. Al-Dhahir, "Beamforming OFDM performance under joint phase noise and I/Q imbalance," *IEEE Trans. Veh. Technol.*, vol. 65, no. 5, pp. 2978–2989, May 2016.

[10] O. Ozdemir, R. Hamila, and N. Al-Dhahir, "Exact average OFDM subcarrier sinr analysis under joint transmit receive I/Q imbalance," *IEEE Trans. Veh. Technol.*, vol. 63, no. 8, pp. 4125–4130, Oct 2014.

[11] M. Lupupa and J. Qi, "I/Q imbalance in generalized frequency division multiplexing under Weibull fading," in *IEEE 26th Annual International Symposium on Personal, Indoor, and Mobile Radio Communications*, Aug 2015, pp. 471–476.

[12] S. Krone and G. Fettweis, "On the capacity of OFDM systems with receiver I/Q imbalance," in *IEEE International Conference on Communications*, May 2008, pp. 1317–1321.

[13] A. Ishaque, P. Sakulkar, and G. Ascheid, "Capacity analysis of uplink multi-user SC-FDMA system with frequency-dependent I/Q imbalance," in *51st Annual Allerton Conference on Communication, Control, and Computing*, Oct 2013, pp. 1067–1074.

[14] B. Selim, P. C. Sofotasios, S. Muhaidat, G. K. Karagiannidis, and B. Sharif, "Performance of differential modulation under rf impairments," in *IEEE International Conference on Communications (ICC)*, May 2017, pp. 1–6.

[15] Y. Zou, M. Valkama, N. Y. Ermolova, and O. Tirkkonen, "Analytical performance of OFDM radio link under RX I/Q imbalance and frequency-selective rayleigh fading channel," in *IEEE 12th International Workshop on Signal Processing Advances in Wireless Communications*, June 2011, pp. 251–255.

[16] A. A. A. Boulogeorgos, P. C. Sofotasios, B. Selim, S. Muhaidat, G. K. Karagiannidis, and M. Valkama, "Effects of rf impairments in communications over cascaded fading channels," *IEEE Trans. Veh. Technol.*, vol. 65, no. 11, pp. 8878–8894, Nov 2016.

[17] C. Zhu, J. Cheng, and N. Al-Dhahir, "Error rate analysis of subcarrier QPSK with receiver I/Q imbalances over Gamma-Gamma fading channels," in *2017 International Conference on Computing, Networking and Communications (ICNC)*, Jan 2017, pp. 88–94.

[18] L. Chen, A. G. Helmy, G. Yue, S. Li, and N. Al-Dhahir, "Performance and compensation of I/Q imbalance in differential STBC-OFDM," in *2016 IEEE Global Communications Conference*, Dec 2016, pp. 1–7.

[19] L. Chen, A. Helmy, G. R. Yue, S. Li, and N. Al-Dhahir, "Performance analysis and compensation of joint TX/RX I/Q imbalance in differential STBC-OFDM," *IEEE Trans. Veh. Technol.*, vol. PP, no. 99, pp. 1–1, 2016.

[20] A. Gouissem, R. Hamila, and M. O. Hasna, "Outage performance of cooperative systems under IQ imbalance," *IEEE Trans. on Commun.*, vol. 62, no. 5, pp. 1480–1489, May 2014.

[21] M. Mokhtar, N. Al-Dhahir, and R. Hamila, "OFDM full-duplex DF relaying under I/Q imbalance and loopback self-interference," *IEEE Trans. Vehicular Technol.*, vol. 65, no. 8, pp. 6737–6741, Aug 2016.

[22] L. Samara, M. Mokhtar, O. Ozdemir, R. Hamila, and T. Khattab, "Residual self-interference analysis for full-duplex OFDM transceivers under phase noise and I/Q imbalance," *IEEE Commun. Lett.*, vol. 21, no. 2, pp. 314–317, Feb 2017.

[23] J. Li, M. Matthaiou, and T. Svensson, "I/Q imbalance in AF dual-hop relaying: Performance analysis in Nakagami-m fading," *IEEE Trans. Commun.*, vol. 62, no. 3, pp. 836–847, March 2014.

[24] ——, "I/Q imbalance in two-way AF relaying," *IEEE Trans. Commun.*, vol. 62, no. 7, pp. 2271–2285, July 2014.

[25] ——, "I/Q imbalance in two-way AF relaying: Performance analysis and detection mode switch," in *IEEE Global Communications Conference (GLOBECOM)*. IEEE, 2014, pp. 4001–4007.

[26] X. Zhang, M. Matthaiou, M. Coldrey, and E. Bjrnson, "Impact of residual transmit RF impairments on training-based MIMO systems," *IEEE Trans. Commun.*, vol. 63, no. 8, pp. 2899–2911, Aug 2015.

[27] N. Kolomvakis, M. Matthaiou, and M. Coldrey, "IQ imbalance in multiuser systems: Channel estimation and compensation," *IEEE Trans. Commun.*, vol. 64, no. 7, pp. 3039–3051, July 2016.

[28] E. Bjornson, M. Matthaiou, and M. Debbah, "Massive MIMO with non-ideal arbitrary arrays: Hardware scaling laws and circuit-aware design," *IEEE Trans. Wireless Commun.*, vol. 14, no. 8, pp. 4353–4368, Aug. 2015.

[29] B. Selim, S. Muhaidat, P. C. Sofotasios, A. Al-Dweik, B. S. Sharif, and T. Stouraitis, "Radio frequency front-end impairments in non-orthogonal multiple access systems," *Submitted to IEEE Veh. Technol. Mag.*, 2017. [Online]. Available: https://www.dropbox.com/s/wivpha5k1hiip58/NOMA.pdf?dl=0

[30] Z. Yang, Z. Ding, P. Fan, and G. K. Karagiannidis, "On the performance of non-orthogonal multiple access systems with partial channel information," *IEEE Trans. Commun.*, vol. 64, no. 2, pp. 654–667, Feb 2016.

[31] Z. Ding, Z. Yang, P. Fan, and H. V. Poor, "On the performance of non-orthogonal multiple access in 5G systems with randomly deployed users," *IEEE Signal Process. Lett.*, vol. 21, no. 12, pp. 1501–1505, Dec 2014.

[32] T. Schenk, *RF imperfections in high-rate wireless systems: impact and digital compensation*. Springer Science & Business Media, 2008.

[33] ——, *RF Imperfections in High-Rate Wireless Systems*. The Netherlands: Springer, 2008.

[34] P. Y. *et al.*, "Single-carrier SM-MIMO: A promising design for broadband large-scale antenna systems," *IEEE Commun. Surveys Tutorials*, vol. 18, no. 3, pp. 1687–1716, thirdquarter 2016.

[35] A. A. Nasir, X. Zhou, S. Durrani, and R. A. Kennedy, "Relaying protocols for wireless energy harvesting and information processing," *IEEE Trans. on Wireless Commun.*, vol. 12, no. 7, pp. 3622–3636, July 2013.

[36] J. Qi, S. Aissa, and M.-S. Alouini, "Impact of I/Q imbalance on the performance of two-way CSI-assisted AF relaying," in *IEEE Wireless Communications and Networking Conf.*, Shanghai, April 2013, pp. 2507–2512.

[37] Y. Saito, Y. Kishiyama, A. Benjebbour, T. Nakamura, A. Li, and K. Higuchi, "Non-orthogonal multiple access (NOMA) for cellular future radio access," in *IEEE 77th Vehicular Technology Conference (VTC Spring)*, June 2013, pp. 1–5.

[38] S. J. Grant and J. K. Cavers, "Analytical calculation of outage probability for a general cellular mobile radio system," in *Gateway to 21st Century Communications Village. VTC 1999-Fall. IEEE VTS 50th Vehicular Technology Conference (Cat. No.99CH36324)*, vol. 3, 1999, pp. 1372–1376 vol.3.

[39] M. Uysal, "Diversity analysis of space-time coding in cascaded Rayleigh fading channels," *IEEE Commun. Lett.*, vol. 10, no. 3, pp. 165–167, Mar 2006.

[40] H. A. David and H. N. Nagaraja, "Order statistics. 2003."